

1 **Quantitative tests of albendazole resistance in beta-tubulin mutants**

2 J.B. Collins<sup>1a</sup>, Skyler A. Stone<sup>2a</sup>, Emily J. Koury<sup>2</sup>, Anna G. Paredes<sup>2</sup>, Fiona Shao<sup>2</sup>, Crystal Lovato<sup>2</sup>, Michael  
3 Chen<sup>2</sup>, Richelle Shi<sup>2</sup>, Anwyn Y. Li<sup>2</sup>, Isa Candal<sup>2</sup>, Khadija Al Moutaa<sup>2</sup>, Nicolas Moya<sup>1</sup> and Erik C. Andersen<sup>1,‡</sup>

4  
5 **Affiliations:**

- 6 1. Department of Biology, Johns Hopkins University, Baltimore, MD, 21218, USA  
7 2. Department of Molecular Biosciences, Northwestern University, Evanston, IL 60208, USA

8  
9 a. Equal contribution

10  
11 **‡Corresponding author:**

12 Erik C. Andersen  
13 Department of Biology  
14 Johns Hopkins University  
15 Bascom UTL 383  
16 3400 North Charles St.  
17 Baltimore, MD 21218  
18 412-516-1282  
19 [erik.andersen@gmail.com](mailto:erik.andersen@gmail.com)

20  
21 **Short Title: Albendazole resistance in beta-tubulin mutants**

22  
23 **Conflicts of interest:** none  
24

25

26 **Abstract:**

27 Benzimidazole (BZ) anthelmintics are among the most important treatments for parasitic nematode  
28 infections in the developing world. Widespread BZ resistance in veterinary parasites and emerging resistance in  
29 human parasites raise major concerns for the continued use of BZs. Knowledge of the mechanisms of resistance  
30 is necessary to make informed treatment decisions and circumvent resistance. Benzimidazole resistance has  
31 traditionally been associated with mutations and natural variants in the *C. elegans* beta-tubulin gene *ben-1* and  
32 orthologs in parasitic species. However, variants in *ben-1* alone do not explain the differences in BZ responses  
33 across parasite populations. Here, we examine the roles of five *C. elegans* beta-tubulin genes (*tbb-1*, *mec-7*,  
34 *tbb-4*, *ben-1*, and *tbb-6*) to identify the role each gene plays in BZ response. We generated *C. elegans* strains  
35 with a loss of each beta-tubulin gene, as well as strains with a loss of *tbb-1*, *mec-7*, *tbb-4*, or *tbb-6* in a genetic  
36 background that also lacks *ben-1* to test beta-tubulin redundancy in BZ response. We found that only the  
37 individual loss of *ben-1* conferred a substantial level of BZ resistance, although the loss of *tbb-1* was found to  
38 confer a small benefit in the presence of albendazole (ABZ). The loss of *ben-1* was found to confer an almost  
39 complete rescue of animal development in the presence of 30  $\mu$ M ABZ, likely explaining why no additive effects  
40 caused by the loss of a second beta-tubulin were observed. We demonstrate that *ben-1* is the only beta-tubulin  
41 gene in *C. elegans* where loss confers substantial BZ resistance.

42  
43 **Keywords:** beta-tubulin, benzimidazole, anthelmintic resistance, *C. elegans*

44  
45  
46  
47  
48  
49  
50  
51  
52  
53  
54  
55  
56  
57  
58  
59  
60  
61  
62

63 **Highlights:**

- 64 - Loss of *ben-1* provides almost complete rescue of development in albendazole (ABZ)
- 65 - Loss of different beta-tubulin genes does not confer ABZ resistance
- 66 - Loss of *ben-1* and a second beta-tubulin does not enhance the *ben-1* level of ABZ resistance

67

68

69

70

71

72

73

74

75

76

77

78

79

80

81

82

83

84

85

86

87

88

89

## 90 1. Introduction

91 Parasitic nematode infections are among the most common infectious diseases of humans and pose  
92 significant health and socioeconomic risks for endemic regions. Upwards of 1.5 billion individuals are estimated  
93 to be infected with at least one parasitic nematode species globally, with infections causing anemia, impaired  
94 cognitive development, reduced growth, diarrheal disease, intestinal obstructions, and lymph edema (Salikin et  
95 al., 2020). Anti-helminth drugs, or anthelmintics, are used in endemic areas to control infections and limit adverse  
96 health effects caused by parasitic nematodes. Anthelmintics are often delivered through mass drug  
97 administration (MDA) programs designed to deliver essential medicines to regions with infected populations.

98 One of the most common anthelmintics delivered in MDA programs is albendazole (ABZ), a drug  
99 belonging to the benzimidazole (BZ) class of anthelmintics. The BZ drug class is included in many MDA programs  
100 because of its broad-spectrum activity, capable of treating a wide variety of intestinal helminths, as well as being  
101 safe and affordable to easily deliver to large populations (Banerjee et al., 2023). Studies of the mode of BZ action  
102 have found that they inhibit the polymerization of microtubules by targeting beta-tubulin (Hastie and  
103 Georgopoulos, 1971; Sheir-Neiss et al., 1978). A study of BZ response in the free-living model nematode  
104 *Caenorhabditis elegans* found that larvae exposed to BZs were developmentally impaired and uncoordinated in  
105 locomotion (Chalfie and Thomson, 1982). Subsequent experiments showed that animals with loss-of-function  
106 mutations in the beta-tubulin gene *ben-1* were found to exhibit wild-type growth and movement in the presence  
107 of BZs (Driscoll et al., 1989). Wild-type growth, despite the loss of *ben-1*, is thought to be possible because  
108 another beta-tubulin gene acts redundantly and compensates for the loss of *ben-1*. The *C. elegans* genome  
109 contains five additional beta-tubulin genes (*tbb-1*, *tbb-2*, *mec-7*, *tbb-4*, and *tbb-6*) that are differentially expressed  
110 in various tissues and are thought to supply beta-tubulin function when *ben-1* is lost (Hurd, 2018).

111 Orthologs of *ben-1* were found to be the target of BZs in parasitic nematodes. A beta-tubulin gene (*tbb-*  
112 *isotype-1*) from *Haemonchus contortus*, a small-ruminant parasite, was found to rescue BZ susceptibility when  
113 expressed in a *C. elegans* strain that lacked *ben-1* (Kwa et al., 1995, 1994, 1993). Unlike *C. elegans*, the *H.*  
114 *contortus* genome contains only four genes encoding beta-tubulins (*tbb-isotype-1*, *tbb-isotype-2*, *tbb-isotype-3*,  
115 and *tbb-isotype-4*). A smaller complement of beta-tubulin genes, combined with expression differences between  
116 each of the four genes has led to the conclusion that loss of *tbb-isotype-1* likely causes lethality, indicating that  
117 BZ resistance in parasites is probably dependent on altered function variants in beta-tubulin. However, parasitic

118 nematodes currently lack the genetic tools, such as genome editing, to validate resistance genes using targeted  
119 mutations. Exploration of anthelmintic resistance is dependent on *C. elegans* as a complement to research in  
120 parasites, and a cycle of discovery has been proposed to explore and validate the mechanisms of BZ resistance  
121 using both free-living and parasitic nematodes (Wit et al., 2021).

122 Anthelmintic resistance is a major concern in the control of parasites. Resistance to the BZ drug class  
123 has become nearly ubiquitous in many nematode species of veterinary importance and is now an emerging  
124 problem in nematode infections of humans (Howell et al., 2008; Kaplan, 2004; Krücken et al., 2017). The  
125 development of resistance to BZs makes the control of infections difficult and costly. To address the emergence  
126 of BZ resistance, it is necessary to understand the underlying genetics contributing to resistance. After suspected  
127 resistance-associated variants are identified in parasites, they can be validated in *C. elegans* using CRISPR-  
128 Cas9 genome editing. Studies of BZ resistance have identified non-synonymous variants at codons 134, 167,  
129 198, and 200 of *ben-1* orthologs in parasites (Avramenko et al., 2019; Kwa et al., 1994; Mohammedsalih et al.,  
130 2020; Venkatesan et al., 2023). Every known beta-tubulin variant associated with BZ resistance in parasitic  
131 nematodes has been shown to cause resistance in *C. elegans* by the introduction of the variant into the *ben-1*  
132 gene (Dilks et al., 2021, 2020; Kitchen et al., 2019; Kwa et al., 1994; Venkatesan et al., 2023). These variants in  
133 parasite beta-tubulin genes are thought to alter a putative BZ binding site, preventing BZs from inhibiting beta-  
134 tubulin, preserving the normal formation of microtubules, and allowing nematodes to survive and develop  
135 normally in the presence of BZ treatment.

136 Despite the validation of variants in *ben-1* orthologs as a mechanism of resistance to BZs, *ben-1* is not  
137 the only gene involved in BZ resistance. Genome-wide association studies in wild populations of *C. elegans*  
138 have identified multiple genomic loci independent of *ben-1* that are associated with BZ resistance (Hahnel et al.,  
139 2018; Zamanian et al., 2018). Fully understanding the genetics of resistance is necessary to inform strategic  
140 decisions that improve the efficacy of existing treatments, as well as lead to the development of new treatments  
141 and control strategies. Thus, it is imperative to identify all genes associated with BZ resistance. Here, we explore  
142 the effects that loss of each beta-tubulin gene has on BZ resistance in *C. elegans*. The gene *ben-1* has been  
143 extensively studied and confers the greatest level of BZ resistance. However, the roles of the other *C. elegans*  
144 beta-tubulin genes (*tbb-1*, *tbb-2*, *mec-7*, *tbb-4*, and *tbb-6*) in BZ resistance are not well understood. We have  
145 compared the effects of single gene deletions of each beta-tubulin gene on nematode development when

146 exposed to a single concentration of ABZ that previously has been found to confer a significant impact on the  
147 development of the wild-type N2 strain of *C. elegans* (Dilks et al., 2021, 2020). We find that the loss of *ben-1*  
148 conferred the highest level of resistance and the loss of *tbb-1* conferred moderate resistance. To test for genetic  
149 redundancy among beta-tubulin genes, we used CRISPR-Cas9 genome editing to delete each beta-tubulin gene  
150 in a genetic background that already has lost *ben-1* function. The loss of each beta-tubulin gene in the *ben-1*  
151 deletion background did not confer a detectable change in ABZ resistance compared to the loss of *ben-1* alone.  
152 Overall, we find that the loss of *ben-1* alone is sufficient to confer the maximum level of *C. elegans* ABZ resistance  
153 at the concentration tested.

## 154

## 155 **2. Materials and Methods**

### 156 **2.1 Generation of phylogeny of selected nematode beta-tubulins**

157 Five nematode species were selected to make a phylogenetic tree of beta-tubulins to observe levels of  
158 conservation. All nematode species selected are Clade V nematodes as the association of *ben-1* orthologs with  
159 BZ resistance has most often been validated in this clade. *C. elegans* and *Caenorhabditis briggsae* were selected  
160 as two closely related free-living nematode species. *Pristionchus pacificus*, another free-living nematode, was  
161 selected because of its high-quality genome and evolutionary divergence from *C. elegans*. Many parasite  
162 genomes are relatively poor quality and lack detailed gene annotations, so we chose two parasite species with  
163 well annotated genomes, the hookworm *Necator americanus* and *H. contortus*, to include in the phylogenetic  
164 tree.

165 *Orthofinder* (Emms and Kelly, 2019) was used to identify beta-tubulin sequences (Supplementary Table  
166 1) from each species. Data were obtained from the following sources: WormBase Parasite (WBPS18) (*H.*  
167 *contortus*, *N. americanus*, *P. pacificus*), WormBase (WS279) (*C. elegans*), and from a previous publication (*C.*  
168 *briggsae*) (Moya et al., 2023). Ortholog sequences were aligned using *Mafft*, and the phylogenetic tree was  
169 generated and annotated using *IQTREE* (Katoch et al., 2002; Minh et al., 2020). *IQTREE* performs automatic  
170 model selection. The selected model was LG+G4, which uses the LG model (Le and Gascuel, 2008) to examine  
171 amino-acid exchange rates and a discrete gamma model with four categories (G4) (Yang, 1994) to examine  
172 heterogeneity across amino acid sites. Branch support was estimated with 1000 iterations of ultrafast bootstrap  
173 approximation (Minh et al., 2013). Putative clades were identified in the generated tree and colored by clade.

174

## 175 **2.2 *C. elegans* strains and maintenance**

176 Nematodes were grown on plates of modified nematode growth media (NGMA) containing 1% agar and  
177 0.7% agarose and seeded with the *Escherichia coli* strain OP50 (Andersen et al., 2014). Plates were maintained  
178 at 20°C for the duration of all experiments. Before each assay, animals were grown for three generations to  
179 reduce the multigenerational effects of starvation.

180 CRISPR-Cas9-edited strains were generated as previously described (Dilks et al., 2020; Hahnel et al.,  
181 2018) (Supplementary File 2), except for VC364 *tbb-1(gk207)*, which was acquired from the *Caenorhabditis*  
182 Genetics Center (Minneapolis, MN). All single deletions were generated in the reference N2 genetic background.  
183 All double deletions were generated in the ECA882 *ben-1(ean64)* genetic background (Dilks et al., 2021, 2020).  
184 Progeny from injected animals (F1) were individually placed onto NGMA plates to reproduce and then sequenced  
185 using Sanger sequencing to confirm the presence of the desired edit. At least two generations of animals after  
186 single-animal passage were Sanger sequenced to confirm successful genome edits. Two independent edits of  
187 each strain were generated to control for any potential off-target effects caused by CRISPR-Cas9.

188

## 189 **2.3 Nematode food preparation**

190 The OP50 strain of *E. coli* was used as a nematode food source on NGMA plates. Bacterial food for the  
191 liquid-based high-throughput assay was prepared as previously described (Widmayer et al., 2022). Briefly, a  
192 frozen stock of the HB101 strain of *E. coli* was used to inoculate and grow a one liter culture at an OD<sub>600</sub> value  
193 of 0.001. Six cultures containing one liter of pre-warmed 1x Horvitz Super Broth (HSB) and an OD<sub>600</sub> inoculum  
194 grew for 15 hours at 37°C until cultures were in the late log growth phase. After 15 hours, flasks were removed  
195 from the incubator and transferred to 4°C to halt bacterial growth. Cultures were pelleted using centrifugation,  
196 the supernatant removed, and washed with K medium. Bacteria were resuspended in K medium, and the OD<sub>600</sub>  
197 value was determined. The bacterial suspension was diluted to a final concentration of OD<sub>600</sub>100 before being  
198 aliquoted to 30 mL and frozen at -80°C.

199

## 200 **2.4 Albendazole stock preparation**

201 A 100  $\mu$ M stock solution of albendazole (Fluka, Catalog #: A4673-10G) was prepared in dimethyl  
202 sulfoxide (DMSO), aliquoted, and stored at  $-20^{\circ}\text{C}$ . A frozen ABZ aliquot was defrosted shortly before adding the  
203 drug to the assay plates.

## 205 **2.5 High-throughput phenotyping assay (HTA)**

206 A previously described HTA was used for all ABZ response phenotyping assays (Shaver et al., 2023).  
207 Two independent assays made up of three bleaches each were performed. Strains underwent three generations  
208 of growth to control for any starvation effects and were then bleach synchronized in triplicate to control for  
209 variation caused by bleach effects. Embryos were concentrated at 0.6 embryos/ $\mu\text{L}$  in 50  $\mu\text{L}$  of K medium (Boyd  
210 et al., 2012). A volume of 50  $\mu\text{L}$  of the embryo solution was dispensed into each well of a 96-well plate. Both  
211 DMSO and ABZ conditions contained 48 wells of N2 and ECA882, and 24 wells of each of the other tested  
212 strains for each replicate bleach. Embryos were allowed to hatch overnight at  $20^{\circ}\text{C}$  with constant shaking at 180  
213 rpm. The following morning, HB101 aliquots were thawed at room temperature, combined, and diluted to  $\text{OD}_{600}30$   
214 with K medium, and kanamycin was added at a concentration of 150  $\mu\text{M}$  to inhibit further bacterial growth and  
215 prevent contamination. The final well concentration of HB101 was  $\text{OD}_{600}10$  and the final concentration of  
216 kanamycin was 50  $\mu\text{M}$ , and each well was treated with either 1% DMSO or 30  $\mu\text{M}$  ABZ in 1% DMSO. Animals  
217 were grown for 48 hours with constant shaking at 180 rpm, after which, animals were treated with 50 mM sodium  
218 azide in M9 buffer to straighten and paralyze the animals for imaging. Following 10 minutes of exposure to  
219 sodium azide, each plate was imaged using a Molecular Devices ImageXpress Nano microscope (Molecular  
220 Devices, San Jose, CA) with a 2X objective (Shaver et al., 2023).

221 Independent assays included identical strain sets except as follows: Strains with a deletion of *tbb-2* were  
222 found to be too developmentally delayed to use in these assays. The ECA3746 *ben-1(ean64); mec-7(ean257)*  
223 strain was removed from assay one because of an insufficient quantity of embryos after bleach synchronization.  
224 Smaller significant effects on animal development were observed for some single deletions in control conditions  
225 of assay one but not in assay two, indicating that significance assigned to the observed small effects could be  
226 the result of high levels of replication, making even small differences significant.

## 228 **2.6 Data cleaning and analysis**



229 High-throughput assay images were processed using CellProfiler  
230 (<https://github.com/AndersenLab/CellProfiler>). Processed image data were cleaned and processed using the  
231 *easyXpress* (Nyaanga et al., 2021) R package as previously described (Shaver et al., 2024). The two assays  
232 were cleaned and processed independently. All statistical comparisons and figure generation were performed in  
233 R(4.1.2) (R Core Team, 2020). We used the *Rstatix* package *tukeyHSD* function on an ANOVA model generated  
234 with the formula *phenotype ~ strain* to calculate differences in the responses of the strains. Figure 3 was  
235 generated using data from assay one because of the large amount of variation shown in animal response for the  
236 VC364 *tbb-1(gk207)* strain in assay two, thought to be caused by human error. Figure 4 was generated using  
237 data from assay two, because of the loss of the ECA3746 strain in assay one. All data are presented in  
238 supplemental figures.

239

### 240 **3. Results**

#### 241 **3.1 Beta-tubulins are well conserved among Clade V nematode species**

242 We wanted to determine how each of the six beta-tubulin genes from *C. elegans* were related to each  
243 other, as well as to orthologs from other nematode species (Hurd, 2018). Phylogenetic analysis found five  
244 putative clades of beta-tubulin proteins (Figure 1). *Caenorhabditis elegans tbb-1* and *tbb-2* share a common  
245 clade with the *tbb-isotype-1* beta-tubulins from *H. contortus* and *N. americanus*. *Caenorhabditis elegans mec-7*  
246 and *tbb-4* are in separate clades with *tbb-isotype-3* and *tbb-isotype-4* clustering with each gene, respectively.  
247 The genes *ben-1* and *tbb-isotype-2* each cluster into separate clades. The gene *tbb-6*, a beta-tubulin unique to  
248 *C. elegans*, could not be placed into the tree because of a high level of divergence. The high levels of  
249 conservation of beta-tubulins among Clade V species highlight the ability to use *C. elegans* as a model system  
250 to investigate the broad roles of beta-tubulins in BZ resistance across diverse nematode species.

251

#### 252 **3.2 The loss of ben-1 is the only beta-tubulin gene to confer high levels of ABZ resistance**

253 CRISPR-Cas9 genome editing was used to generate deletions of each beta-tubulin gene in the N2  
254 laboratory strain genetic background (Figure 2). Edited strains with single deletions of each beta-tubulin gene  
255 were phenotyped in DMSO and ABZ using a previously described high-throughput assay (HTA) that  
256 quantitatively measures nematode development (Shaver et al., 2023; Widmayer et al., 2022). Briefly, strains

257 were bleached synchronized and embryos were titered into 96-well plates. The following day, arrested L1 larvae  
258 were given OP50 *E. coli* with either 1% DMSO or 30  $\mu$ M ABZ and 1% DMSO. Plates were incubated for 48 hours  
259 at 20°C with constant shaking at 180 rpm. Animals were then treated with sodium azide and imaged to quantify  
260 the lengths of each animal in each well of a 96-well plate. Median animal lengths were calculated from each well  
261 of an assay plate and normalized across independent growths, plates, and bleaches. Deletion of each beta-  
262 tubulin gene in the same genetic background enables the determination of the quantitative effects that each  
263 gene has on BZ response, as well as to determine if the loss of each beta-tubulin gene impacts development in  
264 control conditions. Median animal length after 48 hours of exposure was normalized to control conditions, and  
265 then statistical comparisons were made between N2 and each strain. The loss of *tbb-1* had the most significant  
266 impact on development in control conditions, indicating that the loss of *tbb-1* is detrimental (S Figs. 4,6). The  
267 loss of *ben-1* was the only strain to confer high levels of resistance to ABZ, almost fully rescuing development  
268 compared to control conditions (Figure 3, S Figs. 3,5). The loss of *tbb-1* was found to confer a moderate level of  
269 resistance, with animal development significantly less affected than the wild-type strain but still heavily affected  
270 by ABZ as compared to control conditions.

### 271 272 **3.3 The loss of *ben-1* confers the highest level of ABZ resistance compared to other beta-tubulin mutants**

273 To determine if other beta-tubulin genes play a redundant role in ABZ resistance with *ben-1*, we  
274 generated individual deletions of *tbb-1*, *mec-7*, *tbb-4*, and *tbb-6* in the *ben-1(ean64)* genetic background. We  
275 exposed these double beta-tubulin mutants to DMSO and ABZ in the same high-throughput development assay  
276 described above to determine if the loss of a second beta-tubulin alters the levels of BZ resistance observed in  
277 the single *ben-1* mutant. Similarly to the single deletion assay, small significant differences were observed for  
278 multiple strains compared to the wild-type strain in control conditions, except for the strain ECA3628 *ben-1*  
279 *(ean64); tbb-4(ean282)* (S. Figs 8,10), which likely has off-target effects of gene editing that impacted growth  
280 compared to the independently edited second strain. Small differences in the summarized median length reflect  
281 differences in the developmental rate that could be caused by the combined effects of the loss of multiple beta-  
282 tubulins. Strains with the loss of a second beta-tubulin were found to be equally resistant when compared to the  
283 loss of *ben-1* alone (Figure 4, S Figs. 7,9). As previously noted, the loss of *ben-1* almost fully rescued

development at 30  $\mu$ M ABZ compared to the control strain, possibly preventing any small effects conferred by the loss of a second beta-tubulin from being observed.

## 4. Discussion

Despite the role beta-tubulin variants have in BZ resistance, the collective understanding of BZ resistance comes from studies of *C. elegans ben-1* and orthologs in parasites. Fully understanding the mechanisms underlying BZ resistance is imperative to the future of BZs as anthelmintic treatments. Here, we take an important first step to test additional beta-tubulin genes in BZ resistance.

### 4.1 *ben-1* plays the largest role in ABZ resistance in *C. elegans*

We examined the role that five of the six *C. elegans* beta-tubulin genes play in ABZ resistance by generating strains with a loss of each gene, as well as strains with a loss of an additional beta-tubulin in a *ben-1* mutant background. Because of detrimental effects on development, strains with a loss of *tbb-2* could not be measured for responses to ABZ. Consistent with previous studies, the loss of *ben-1* was sufficient to confer the maximum level of ABZ resistance, though it is important to note that the loss of *tbb-1* conferred a moderate level of resistance. Loss of a second beta-tubulin in a strain with a loss of *ben-1* did not confer a detectable enhancement of resistance. However, we can not definitively conclude if any other beta-tubulin gene acts redundantly with *ben-1* in ABZ resistance. The assay that we used to measure ABZ resistance uses one concentration that previously was found to differentiate susceptible strains from *ben-1* mutant strains (Dilks et al., 2021, 2020). It remains possible that enhancement of ABZ resistance could be detected at higher ABZ concentrations where the single contribution of *ben-1* might not be sufficient to cause resistance alone. Another caveat is that only a single trait, development, was measured. ABZ affects multiple traits, including fecundity and competitive fitness over multiple generations (Shaver et al., 2024). Future studies should investigate multiple traits at different ABZ concentrations to fully understand the role of all beta-tubulin genes in the ABZ response.

### 4.2 BZ resistance is complicated by differences in beta-tubulin copy number, levels of expression, and resistance alleles

311 We tested the role of each beta-tubulin gene in ABZ response by deleting much of the coding sequence.  
312 Therefore, these results are binary for the presence or absence of each beta-tubulin gene. Amino-acid altering  
313 variants from parasites have been validated in ABZ resistance using *C. elegans* and shown to cause ABZ  
314 resistance equivalent to a strain with a loss of *ben-1* (Dilks et al., 2021, 2020; Venkatesan et al., 2023). However,  
315 these variants likely do not cause loss of *tbb-isotype-1* function in parasites (Saunders et al., 2013). What could  
316 be causing this discrepancy between loss-of-function variants in *C. elegans* and potential altered function  
317 variants in parasitic nematodes? In species with highly expressed beta-tubulin genes that have BZ-sensitive  
318 alleles, loss-of-function alleles would cause fitness defects, similar to what we see with *tbb-1* and *tbb-2* (Figure  
319 4). In these species, benzimidazole resistance must be mediated by altered function variants. In species with  
320 less highly expressed (or tissue-specific) beta-tubulin genes that have BZ-sensitive alleles, loss-of-function  
321 alleles could cause BZ resistance because other beta-tubulin genes can substitute for essential functions, similar  
322 to what we see with *ben-1* (Hurd, 2018). Interestingly, the *H. contortus* beta-tubulin gene *tbb-isotype-2* is shown  
323 to be equally related to *tbb-isotype-1* and *ben-1*, and loss-of-function alleles of this gene have been documented  
324 in some highly resistant *H. contortus* populations (Saunders et al., 2013). Additionally, the phenotypic  
325 classification of BZ-resistance phenotypes differs between these two species and can be explained by  
326 differences in loss-of-function vs. altered function mutations. In *C. elegans* where *ben-1* variants or mutations  
327 can cause loss of function, the BZ-resistance phenotype is recessive (Dilks et al., 2021). By contrast, putative  
328 BZ-resistance alleles in *H. contortus* are hypothesized to cause dominant BZ resistance (Silvestre et al., 2001).

329  
330 Beyond coding variants or mutations in beta-tubulin genes, changes in the levels and tissue-specific  
331 expression can alter BZ resistance. Previously, we found that some *C. elegans* wild strains with clear ABZ  
332 resistance do not have variants that alter the coding sequence of *ben-1* but instead have much lower expression  
333 levels of *ben-1* as compared to the rest of the population (Zhang et al., 2022). These strains are resistant because  
334 the susceptible beta-tubulin protein is not expressed. Additionally, we found that the expression of *ben-1* in  
335 cholinergic neurons alone is sufficient to confer susceptibility to ABZ (Gibson et al., 2022), highlighting that  
336 variants modifying expression in specific tissues could confer resistance in a unique way independent of the  
337 beta-tubulin coding sequence. These observations from both *C. elegans* and *H. contortus* demonstrate that more  
338 attention should be paid to the number of beta-tubulin genes, their levels of expression, the sites of expression,

339 and the putative BZ-resistance alleles found in each beta-tubulin gene. To definitively understand BZ resistance  
340 mediated by beta-tubulin genes, we must also drastically improve parasitic nematode genomes and gene models  
341 because most species lack full descriptions of their beta-tubulin complement.

## 343 5. Future directions

344 The role of *ben-1* and *tbb-isotype-1* beta-tubulins in BZ resistance has been thought to be similar and  
345 has established *C. elegans* as an essential model for parasite BZ resistance research. However, BZ treatment  
346 is typically fatal in susceptible parasites (Prichard, 1988), as well as documented ovicidal effects of BZs against  
347 parasite embryos (Boes et al., 1998). Conversely, the same effects are not typically seen in *C. elegans* where  
348 the most significant impact is often on the developmental rate (Shaver et al., 2022). The loss of *tbb-1* or *tbb-2*  
349 was deleterious and loss-of-function mutations in either gene would likely be rapidly selected against in the wild  
350 (*i.e.*, no variants are observed in natural *C. elegans* strains) (Crombie et al., 2024), similarly to the predicted loss  
351 of *tbb-isotype-1*. It is important to note that *tbb-1* and *tbb-2* have known resistance alleles at amino acid position  
352 200, and future studies should edit both genes to make them harbor BZ-sensitive alleles to more closely  
353 approximate the beta-tubulin complement and alleles in *H. contortus*. Such studies could offer an improved  
354 model system for investigating BZ resistance. However, studies of BZ resistance need to investigate variants  
355 beyond single amino-acid alterations. Our results demonstrate that a variety of factors such as copy number,  
356 expression, and tissue-specific function can all affect BZ resistance. To continue to broaden our understanding  
357 of BZ resistance, we must expand to a whole-genome approach that investigates variants across every single  
358 beta-tubulin gene and beyond that single class of genes.

## 361 **Data Availability**

362 All code and data are openly available at [https://github.com/AndersenLab/2024\\_beta\\_tubulin\\_manuscript](https://github.com/AndersenLab/2024_beta_tubulin_manuscript)

## 364 **Acknowledgments**

365 We would like to thank members of the Andersen lab for their feedback in the preparation of this manuscript. We  
366 thank the *Caenorhabditis* Natural Diversity Resource (NSF Capacity Grant 2224885) and the *Caenorhabditis*  
367 Genetics Center (NIH Office of Research Infrastructure Programs, P40 OD010440) for providing the strains used  
368 in this study. Additionally, we would also like to thank WormBase for providing an essential resource for genetic  
369 and genomic data used in this manuscript.

## 371 **Funding Sources**

372 Skyler Stone, Fiona Shao, and Gracie Paredes were funded by Northwestern University Summer Undergraduate  
373 Research Grants. Skyler Stone was also funded by the Posner Research Program at Northwestern University.  
374 This work was supported by the National Institutes of Health NIAID grant R01AI153088 to ECA.

## 376 **References**

- 377 Andersen, E.C., Bloom, J.S., Gerke, J.P., Kruglyak, L., 2014. A variant in the neuropeptide receptor npr-1 is a  
378 major determinant of *Caenorhabditis elegans* growth and physiology. *PLoS Genet.* 10, e1004156.
- 379 Avramenko, R.W., Redman, E.M., Melville, L., Bartley, Y., Wit, J., Queiroz, C., Bartley, D.J., Gilleard, J.S.,  
380 2019. Deep amplicon sequencing as a powerful new tool to screen for sequence polymorphisms  
381 associated with anthelmintic resistance in parasitic nematode populations. *Int. J. Parasitol.* 49, 13–26.
- 382 Banerjee, S., Mukherjee, S., Nath, P., Mukherjee, A., Mukherjee, S., Ashok Kumar, S.K., De, S., Banerjee, S.,  
383 2023. A critical review of benzimidazole: Sky-high objectives towards the lead molecule to predict the  
384 future in medicinal chemistry. *Results in Chemistry* 6, 101013.
- 385 Boes, J., Eriksen, L., Nansen, P., 1998. Embryonation and infectivity of *Ascaris suum* eggs isolated from  
386 worms expelled by pigs treated with albendazole, pyrantel pamoate, ivermectin or piperazine  
387 dihydrochloride. *Vet. Parasitol.* 75, 181–190.
- 388 Boyd, W.A., Smith, M.V., Freedman, J.H., 2012. *Caenorhabditis elegans* as a Model in Developmental  
389 Toxicology, in: Harris, C., Hansen, J.M. (Eds.), *Developmental Toxicology: Methods and Protocols*.  
390 Humana Press, Totowa, NJ, pp. 15–24.
- 391 Chalfie, M., Thomson, J.N., 1982. Structural and functional diversity in the neuronal microtubules of  
392 *Caenorhabditis elegans*. *J. Cell Biol.* 93, 15–23.
- 393 Crombie, T.A., McKeown, R., Moya, N.D., Evans, K.S., Widmayer, S.J., LaGrassa, V., Roman, N., Tursunova,  
394 O., Zhang, G., Gibson, S.B., Buchanan, C.M., Roberto, N.M., Vieira, R., Tanny, R.E., Andersen, E.C.,  
395 2024. CaenNDR, the *Caenorhabditis* Natural Diversity Resource. *Nucleic Acids Res.* 52, D850–D858.
- 396 Dilks, C.M., Hahnel, S.R., Sheng, Q., Long, L., McGrath, P.T., Andersen, E.C., 2020. Quantitative  
397 benzimidazole resistance and fitness effects of parasitic nematode beta-tubulin alleles. *Int. J. Parasitol.*  
398 *Drugs Drug Resist.* 14, 28–36.
- 399 Dilks, C.M., Koury, E.J., Buchanan, C.M., Andersen, E.C., 2021. Newly identified parasitic nematode beta-  
400 tubulin alleles confer resistance to benzimidazoles. *Int. J. Parasitol. Drugs Drug Resist.* 17, 168–175.



- 401 Driscoll, M., Dean, E., Reilly, E., Bergholz, E., Chalfie, M., 1989. Genetic and molecular analysis of a  
402 *Caenorhabditis elegans* beta-tubulin that conveys benzimidazole sensitivity. *J. Cell Biol.* 109, 2993–3003.
- 403 Emms, D.M., Kelly, S., 2019. OrthoFinder: phylogenetic orthology inference for comparative genomics.  
404 *Genome Biol.* 20, 238.
- 405 Gibson, S.B., Ness-Cohn, E., Andersen, E.C., 2022. Benzimidazoles cause lethality by inhibiting the function of  
406 *Caenorhabditis elegans* neuronal beta-tubulin. *Int. J. Parasitol. Drugs Drug Resist.* 20, 89–96.
- 407 Hahnel, S.R., Zdraljevic, S., Rodriguez, B.C., Zhao, Y., McGrath, P.T., Andersen, E.C., 2018. Extreme allelic  
408 heterogeneity at a *Caenorhabditis elegans* beta-tubulin locus explains natural resistance to  
409 benzimidazoles. *PLoS Pathog.* 14, e1007226.
- 410 Hastie, A.C., Georgopoulos, S.G., 1971. Mutational resistance to fungitoxic benzimidazole derivatives in  
411 *Aspergillus nidulans*. *J. Gen. Microbiol.* 67, 371–373.
- 412 Howell, S.B., Burke, J.M., Miller, J.E., Terrill, T.H., Valencia, E., Williams, M.J., Williamson, L.H., Zajac, A.M.,  
413 Kaplan, R.M., 2008. Prevalence of anthelmintic resistance on sheep and goat farms in the southeastern  
414 United States. *J. Am. Vet. Med. Assoc.* 233, 1913–1919.
- 415 Hurd, D.D., 2018. Tubulins in *C. elegans*. *WormBook*.
- 416 Kaplan, R.M., 2004. Drug resistance in nematodes of veterinary importance: a status report. *Trends Parasitol.*  
417 20, 477–481.
- 418 Katoh, K., Misawa, K., Kuma, K.-I., Miyata, T., 2002. MAFFT: a novel method for rapid multiple sequence  
419 alignment based on fast Fourier transform. *Nucleic Acids Res.* 30, 3059–3066.
- 420 Kitchen, S., Ratnappan, R., Han, S., Leasure, C., Grill, E., Iqbal, Z., Granger, O., O’Halloran, D.M., Hawdon,  
421 J.M., 2019. Isolation and characterization of a naturally occurring multidrug-resistant strain of the canine  
422 hookworm, *Ancylostoma caninum*. *Int. J. Parasitol.* 49, 397–406.
- 423 Krücken, J., Fraundorfer, K., Mugisha, J.C., Ramünke, S., Sifft, K.C., Geus, D., Habarugira, F., Ndoli, J.,  
424 Sendegeya, A., Mukampunga, C., Bayingana, C., Aebischer, T., Demeler, J., Gahutu, J.B., Mockenhaupt,  
425 F.P., von Samson-Himmelstjerna, G., 2017. Reduced efficacy of albendazole against *Ascaris lumbricoides*  
426 in Rwandan schoolchildren. *Int. J. Parasitol. Drugs Drug Resist.* 7, 262–271.
- 427 Kwa, M.S., Kooyman, F.N., Boersema, J.H., Roos, M.H., 1993. Effect of selection for benzimidazole resistance  
428 in *Haemonchus contortus* on beta-tubulin isotype 1 and isotype 2 genes. *Biochem. Biophys. Res.*  
429 *Commun.* 191, 413–419.
- 430 Kwa, M.S., Veenstra, J.G., Roos, M.H., 1994. Benzimidazole resistance in *Haemonchus contortus* is correlated  
431 with a conserved mutation at amino acid 200 in beta-tubulin isotype 1. *Mol. Biochem. Parasitol.* 63, 299–  
432 303.
- 433 Kwa, M.S., Veenstra, J.G., Van Dijk, M., Roos, M.H., 1995. Beta-tubulin genes from the parasitic nematode  
434 *Haemonchus contortus* modulate drug resistance in *Caenorhabditis elegans*. *J. Mol. Biol.* 246, 500–510.
- 435 Le, S.Q., Gascuel, O., 2008. An improved general amino acid replacement matrix. *Mol. Biol. Evol.* 25, 1307–  
436 1320.
- 437 Minh, B.Q., Nguyen, M.A.T., von Haeseler, A., 2013. Ultrafast approximation for phylogenetic bootstrap. *Mol.*  
438 *Biol. Evol.* 30, 1188–1195.
- 439 Minh, B.Q., Schmidt, H.A., Chernomor, O., Schrempf, D., Woodhams, M.D., von Haeseler, A., Lanfear, R.,  
440 2020. IQ-TREE 2: New Models and Efficient Methods for Phylogenetic Inference in the Genomic Era. *Mol.*  
441 *Biol. Evol.* 37, 1530–1534.
- 442 Mohammedsalih, K.M., Krücken, J., Khalafalla, A., Bashar, A., Juma, F.-R., Abakar, A., Abdalmalaik, A.A.H.,  
443 Coles, G., von Samson-Himmelstjerna, G., 2020. New codon 198  $\beta$ -tubulin polymorphisms in highly  
444 benzimidazole resistant *Haemonchus contortus* from goats in three different states in Sudan. *Parasit.*  
445 *Vectors* 13, 114.
- 446 Moya, N.D., Stevens, L., Miller, I.R., Sokol, C.E., Galindo, J.L., Bardas, A.D., Koh, E.S.H., Rozenich, J., Yeo,  
447 C., Xu, M., Andersen, E.C., 2023. Novel and improved *Caenorhabditis briggsae* gene models generated  
448 by community curation. *bioRxiv*. <https://doi.org/10.1101/2023.05.16.541014>
- 449 Nyaanga, J., Crombie, T.A., Widmayer, S.J., Andersen, E.C., 2021. easyXpress: An R package to analyze and  
450 visualize high-throughput *C. elegans* microscopy data generated using CellProfiler. *PLoS One* 16,  
451 e0252000.
- 452 Prichard, R.K., 1988. Anthelmintics and control. *Vet. Parasitol.* 27, 97–109.
- 453 R Core Team, 2020. R: A Language and Environment for Statistical Computing.
- 454 Salikin, N.H., Nappi, J., Majzoub, M.E., Egan, S., 2020. Combating Parasitic Nematode Infections, Newly  
455 Discovered Antinematode Compounds from Marine Epiphytic Bacteria. *Microorganisms* 8.  
456 <https://doi.org/10.3390/microorganisms8121963>

- 457 Saunders, G.I., Wasmuth, J.D., Beech, R., Laing, R., Hunt, M., Naghra, H., Cotton, J.A., Berriman, M., Britton,  
458 C., Gilleard, J.S., 2013. Characterization and comparative analysis of the complete *Haemonchus*  
459 *contortus*  $\beta$ -tubulin gene family and implications for benzimidazole resistance in strongylid nematodes. *Int.*  
460 *J. Parasitol.* 43, 465–475.
- 461 Shaver, A.O., Miller, I.R., Schaye, E.S., Moya, N.D., Collins, J.B., Wit, J., Blanco, A.H., Shao, F.M., Andersen,  
462 E.J., Khan, S.A., Paredes, G., Andersen, E.C., 2024. Quantifying the fitness effects of resistance alleles  
463 with and without anthelmintic selection pressure using *Caenorhabditis elegans*. *bioRxiv*.  
464 <https://doi.org/10.1101/2024.02.01.578300>
- 465 Shaver, A.O., Wit, J., Dilks, C.M., Crombie, T.A., Li, H., Aroian, R.V., Andersen, E.C., 2023. Variation in  
466 anthelmintic responses are driven by genetic differences among diverse *C. elegans* wild strains. *PLoS*  
467 *Pathog.* 19, e1011285.
- 468 Shaver, A.O., Wit, J., Dilks, C.M., Crombie, T.A., Li, H., Aroian, R.V., Andersen, E.C., 2022. Variation in  
469 anthelmintic responses are driven by genetic differences among diverse *C. elegans* wild strains. *bioRxiv*.  
470 <https://doi.org/10.1101/2022.11.26.518036>
- 471 Sheir-Neiss, G., Lai, M.H., Morris, N.R., 1978. Identification of a gene for beta-tubulin in *Aspergillus nidulans*.  
472 *Cell* 15, 639–647.
- 473 Silvestre, A., Cabaret, J., Humbert, J.F., 2001. Effect of benzimidazole under-dosing on the resistant allele  
474 frequency in *Teladorsagia circumcincta* (Nematoda). *Parasitology* 123, 103–111.
- 475 Venkatesan, A., Jimenez Castro, P.D., Morosetti, A., Horvath, H., Chen, R., Redman, E., Dunn, K., Collins,  
476 J.B., Fraser, J.S., Andersen, E.C., Kaplan, R.M., Gilleard, J.S., 2023. Molecular evidence of widespread  
477 benzimidazole drug resistance in *Ancylostoma caninum* from domestic dogs throughout the USA and  
478 discovery of a novel  $\beta$ -tubulin benzimidazole resistance mutation. *PLoS Pathog.* 19, e1011146.
- 479 Widmayer, S.J., Crombie, T.A., Nyaanga, J.N., Evans, K.S., Andersen, E.C., 2022. *C. elegans* toxicant  
480 responses vary among genetically diverse individuals. *Toxicology* 479, 153292.
- 481 Wit, J., Dilks, C.M., Andersen, E.C., 2021. Complementary Approaches with Free-living and Parasitic  
482 Nematodes to Understanding Anthelmintic Resistance. *Trends Parasitol.* 37, 240–250.
- 483 Yang, Z., 1994. Maximum likelihood phylogenetic estimation from DNA sequences with variable rates over  
484 sites: approximate methods. *J. Mol. Evol.* 39, 306–314.
- 485 Zamanian, M., Cook, D.E., Zdraljevic, S., Brady, S.C., Lee, D., Lee, J., Andersen, E.C., 2018. Discovery of  
486 genomic intervals that underlie nematode responses to benzimidazoles. *PLoS Negl. Trop. Dis.* 12,  
487 e0006368.
- 488 Zhang, G., Roberto, N.M., Lee, D., Hahnel, S.R., Andersen, E.C., 2022. The impact of species-wide gene  
489 expression variation on *Caenorhabditis elegans* complex traits. *Nat. Commun.* 13, 3462.

## 490 **Legends to Figures**

491 **Figure 1. Phylogenetic relationship of nematode beta-tubulins.** Beta-tubulin gene models from three free-  
492 living nematodes, *Caenorhabditis elegans* (*C.e.*), *C. briggsae* (*C.b.*), and *Pristionchus pacificus* (*P.p.*), and two  
493 parasitic nematodes, *Haemonchus contortus* (*H.c.*) and *Necator americanus* (*N.a.*), were used to generate a  
494 tree showing the relationship between beta-tubulin genes. Branches are colored by putatively assigned clades.  
495 Sequence data were obtained from the following sources: WormBase Parasite (WBPS18) (*H. contortus*, *N.*  
496 *americanus*, *P. pacificus*), WormBase (WS279) (*C. elegans*), and from a previous publication (*C. briggsae*)  
497 (Moya et al. 2023).  
498  
499

500 **Figure 2. Gene models and locations of deletion alleles generated in *C. elegans* beta-tubulin genes.** Gene  
501 models of the longest isoforms are presented for each *C. elegans* beta-tubulin gene, with exons (orange), introns  
502 (gray lines), and untranscribed regions (gray boxes) shown. Regions that were deleted using CRISPR-Cas9  
503 genome editing are shown as black lines under each model. Deleted regions of *tbb-1* are shown as two black  
504 lines because strains with two independent deletion alleles were used. Gene model data were obtained from  
505 WormBase (WS279).  
506

507 **Figure 3. Only loss of *ben-1* causes resistance to ABZ.** Median animal lengths of strains grown in 30  $\mu$ M ABZ  
508 that have been regressed for bleach effects and then normalized to the mean of all median animal lengths from  
509 the control condition are shown. Each point represents the summarized measurements of an individual well  
510 containing five to 30 animals. Data are shown as box plots with the median as a solid horizontal line and the  
511 75th and 25th quartiles on the top and bottom of the box, respectively. The top and bottom whiskers extend to



the maximum point within the 1.5 interquartile range from the 75th and 25th quartiles, respectively. Statistical significance compared to the wild-type strain is shown above each strain ( $p < 0.05 = *$ ,  $p < 0.0001 = ****$ , ANOVA with Tukey HSD).

**Figure 4. None of the other beta-tubulin genes act redundantly with *ben-1* in ABZ response.** Median animal lengths of strains grown in 30  $\mu$ M ABZ that have been regressed for bleach effects and then normalized to the mean of all median animal lengths from the control condition are shown. Each point represents the summarized measurements of an individual well containing five to 30 animals. Data are shown as box plots with the median as a solid horizontal line and the 75th and 25th quartiles on the top and bottom of the box, respectively. The top and bottom whiskers extend to the maximum point within the 1.5 interquartile range from the 75th and 25th quartiles, respectively. Statistical significance compared to the  $\Delta ben-1$  strain is shown above each strain ( $p < 0.05 = *$ ,  $p < 0.0001 = ****$ , ANOVA with Tukey HSD).

**Supplemental Figure 1. Distribution of raw animal lengths for each strain in assay two after exposure to ABZ.** Raw median animal lengths, summarized by well, for each strain are shown for DMSO (0  $\mu$ M) and ABZ (30  $\mu$ M) conditions. Wells are colored by the corresponding replicate bleach synchronization (red=1, green=2, blue=3).

**Supplemental Figure 2. Distribution of raw animal lengths for each strain in assay one after exposure to ABZ.** Raw median animal lengths, summarized by well, for each strain are shown for DMSO (0  $\mu$ M) and ABZ (30  $\mu$ M) conditions. Wells are colored by the corresponding replicate bleach synchronization (red=1, green=2, blue=3).

**Supplemental Figure 3. Only loss of *ben-1* causes ABZ resistance.** Median animal lengths of strains grown in 30  $\mu$ M ABZ that have been regressed for bleach effects and then normalized to the mean of all median animal lengths from the control condition are shown. Each point represents the summarized measurements of an individual well containing five to 30 animals. Data are shown as box plots with the median as a solid horizontal line and the 75th and 25th quartiles on the top and bottom of the box, respectively. The top and bottom whiskers extend to the maximum point within the 1.5 interquartile range from the 75th and 25th quartiles, respectively. Statistical significance compared to the wild-type strain is shown above each strain ( $p < 0.05 = *$ ,  $p < 0.0001 = ****$ , ANOVA with Tukey HSD).

**Supplemental Figure 4. Loss of beta-tubulin genes affects animal lengths in control conditions.** Median animal lengths of strains grown in 1% DMSO are shown. Each point represents the summarized measurements of an individual well containing five to 30 animals. Data are shown as box plots with the median as a solid horizontal line and the 75th and 25th quartiles on the top and bottom of the box, respectively. The top and bottom whiskers extend to the maximum point within the 1.5 interquartile range from the 75th and 25th quartiles, respectively. Statistical significance compared to the wild-type strain is shown above each strain ( $p < 0.05 = *$ ,  $p < 0.0001 = ****$ , ANOVA with Tukey HSD).

**Supplemental Figure 6. Loss of beta-tubulin genes affects animal lengths in control conditions.** Median animal lengths of strains grown in 1% DMSO are shown. Each point represents the summarized measurements of an individual well containing five to 30 animals. Data are shown as box plots with the median as a solid horizontal line and the 75th and 25th quartiles on the top and bottom of the box, respectively. The top and bottom whiskers extend to the maximum point within the 1.5 interquartile range from the 75th and 25th quartiles, respectively. Statistical significance compared to the wild-type strain is shown above each strain ( $p < 0.05 = *$ ,  $p < 0.0001 = ****$ , ANOVA with Tukey HSD).

**Supplemental Figure 7. Additional loss of beta-tubulin genes in a  $\Delta ben-1$  background did not confer a detectable level of increased ABZ resistance.** Median animal lengths of strains grown in 30  $\mu$ M ABZ that have been regressed for bleach effects and then normalized to the mean of all median animal lengths from the control condition are shown. Each point represents the summarized measurements of an individual well containing five to 30 animals. Data are shown as box plots with the median as a solid horizontal line and the 75th and 25th quartiles on the top and bottom of the box, respectively. The top and bottom whiskers extend to the maximum point within the 1.5 interquartile range from the 75th and 25th quartiles, respectively. Statistical significance

567 compared to the  $\Delta ben-1$  strain is shown above each strain ( $p < 0.05 = *$ ,  $p < 0.0001 = ****$ , ANOVA with Tukey  
568 HSD).  
569

570 **Supplemental Figure 8. Loss of multiple beta-tubulins affects animal lengths in control conditions.**

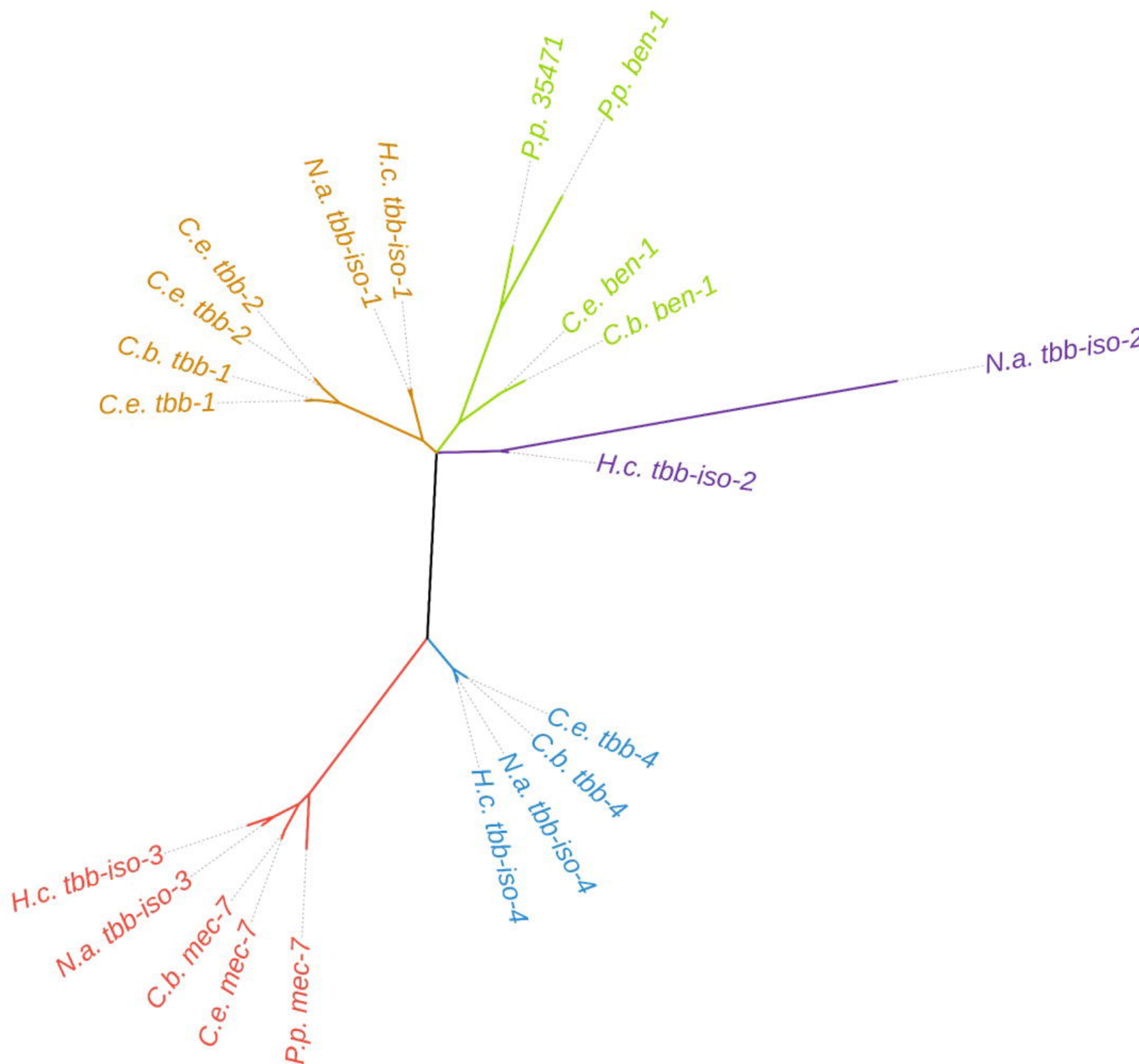
571 Median animal lengths of strains grown in 1% DMSO are shown. Each point represents the summarized  
572 measurements of an individual well containing five to 30 animals. Where applicable, data from both independent  
573 edits in Assay 2 are shown. Data are shown as box plots with the median as a solid horizontal line, with the 75th  
574 and 25th quartiles on the top and bottom of the box, respectively. The top and bottom whiskers extend to the  
575 maximum point within the 1.5 interquartile range from the 75th and 25th quartiles, respectively. Statistical  
576 significance compared to the wild-type strain is shown above each strain ( $p < 0.05 = *$ ,  $p < 0.001 = **$ ,  $p < 0.0001$   
577  $= ****$ , ANOVA with Tukey HSD).  
578

579 **Supplemental Figure 9. Additional loss of beta-tubulin genes in a  $\Delta ben-1$  background did not confer a  
580 detectable level of increased ABZ resistance.**

581 Median animal lengths of strains grown in 30  $\mu\text{M}$  ABZ that have been regressed for bleach effects and then normalized to the mean of all median animal lengths from the control  
582 condition are shown. Each point represents the summarized measurements of an individual well containing five  
583 to 30 animals. Data from both independent edits in Assay 1 are shown. Data are shown as box plots with the  
584 median as a solid horizontal line, with the 75th and 25th quartiles on the top and bottom of the box, respectively.  
585 The top and bottom whiskers extend to the maximum point within 1.5 interquartile range from the 75th and 25th  
586 quartiles, respectively. Statistical significance compared to the  $\Delta ben-1$  strain is shown above each strain ( $p <$   
587  $0.05 = *$ ,  $p < 0.001 = **$ ,  $p < 0.0001 = ****$ , ANOVA with Tukey HSD).  
588

589 **Supplemental Figure 10. Loss of multiple beta-tubulin genes affects animal lengths in control conditions.**

590 Median animal lengths of strains grown in 1% DMSO are shown. Each point represents the summarized  
591 measurements of an individual well containing five to 30 animals. Data are shown as box plots with the median  
592 as a solid horizontal line and the 75th and 25th quartiles on the top and bottom of the box, respectively. The top  
593 and bottom whiskers extend to the maximum point within the 1.5 interquartile range from the 75th and 25th  
594 quartiles, respectively. Statistical significance compared to the wild-type strain is shown above each strain ( $p <$   
595  $0.05 = *$ ,  $p < 0.001 = **$ ,  $p < 0.0001 = ****$ , ANOVA with Tukey HSD).  
596



*rbb-1*



*rbb-2*



*mec-7*



*rbb-4*



*ben-1*



*rbb-6*



0

1

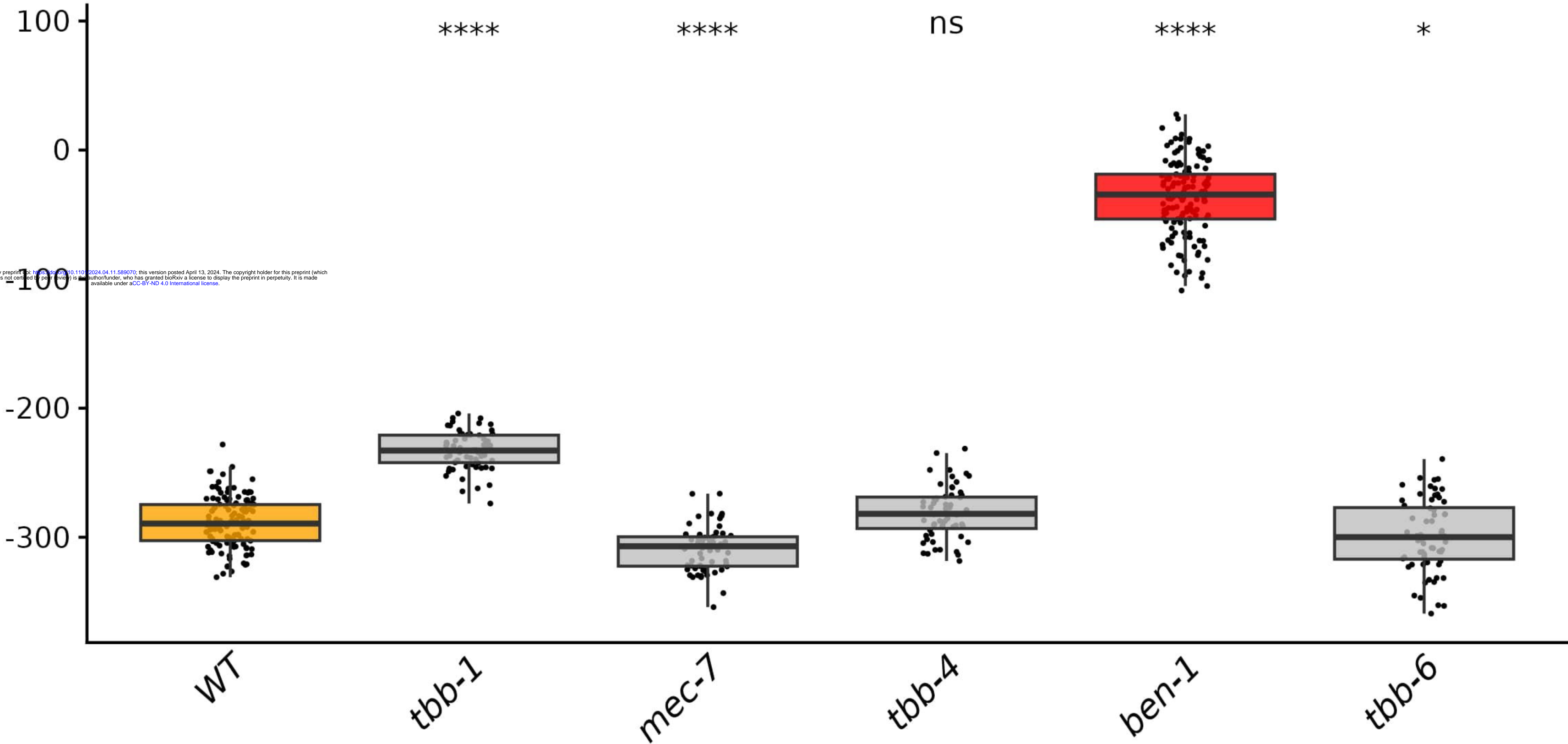
2

3

4

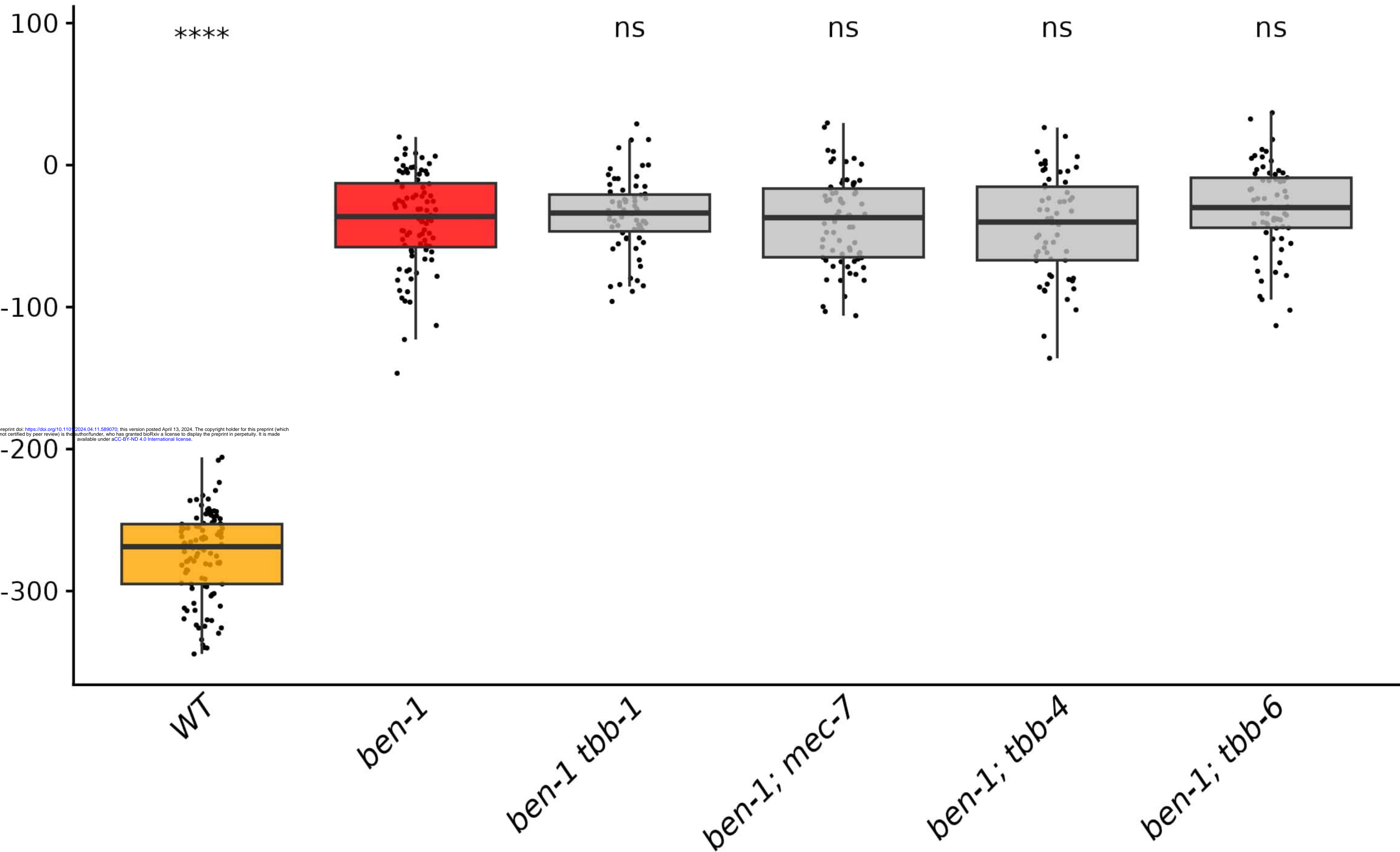
Transcript length (kb)

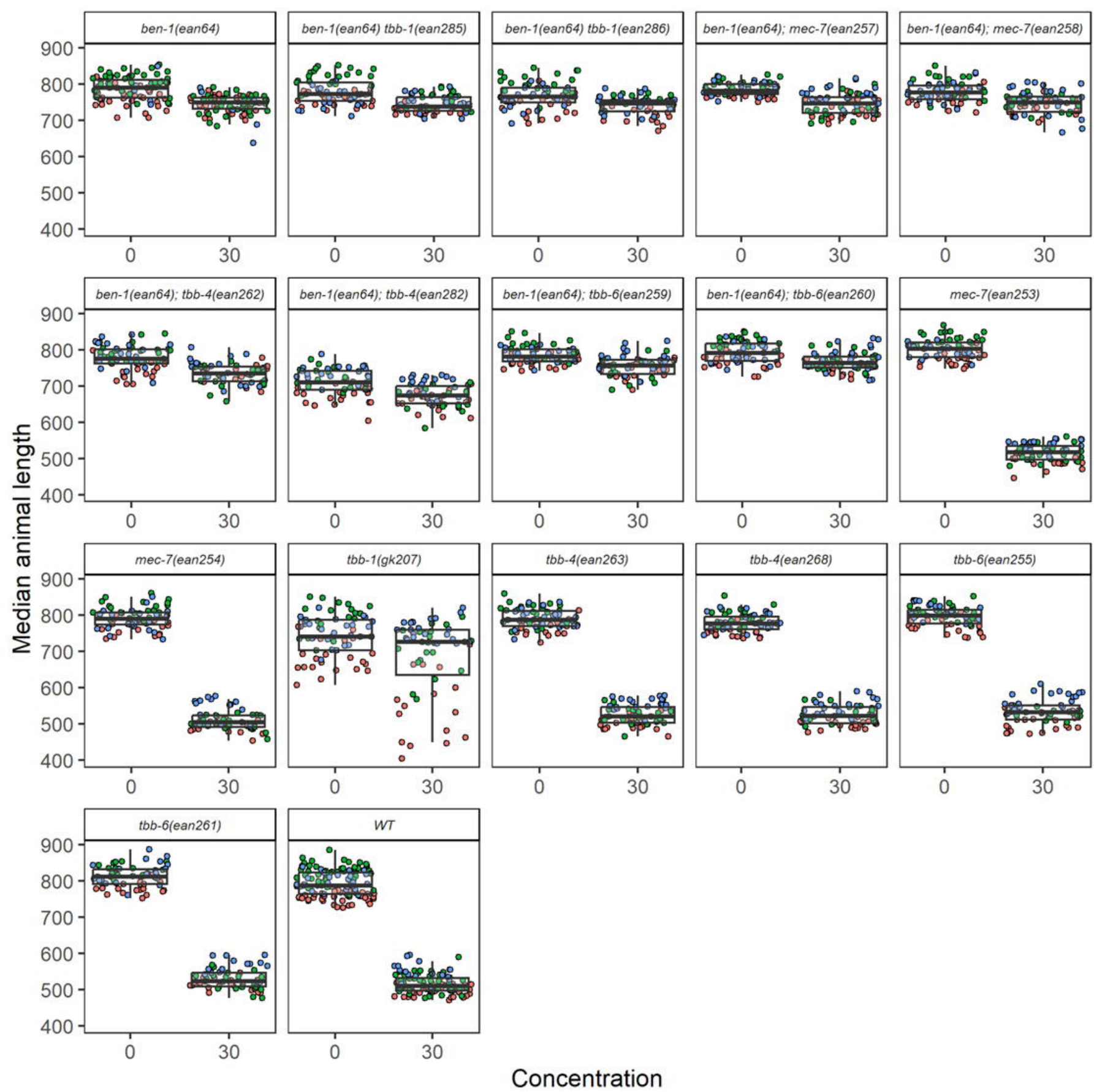
Normalized median animal length



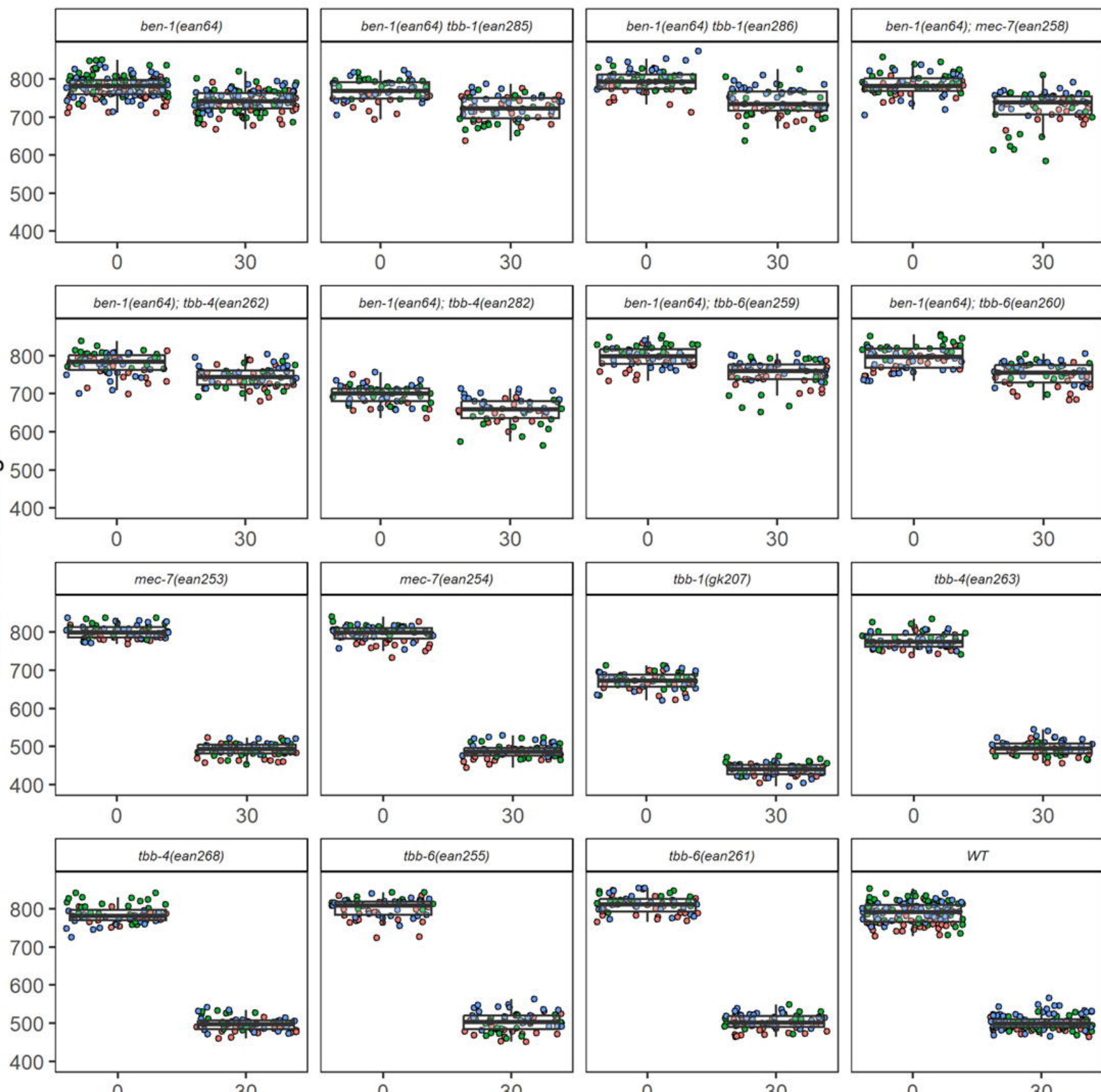


Normalized median animal length



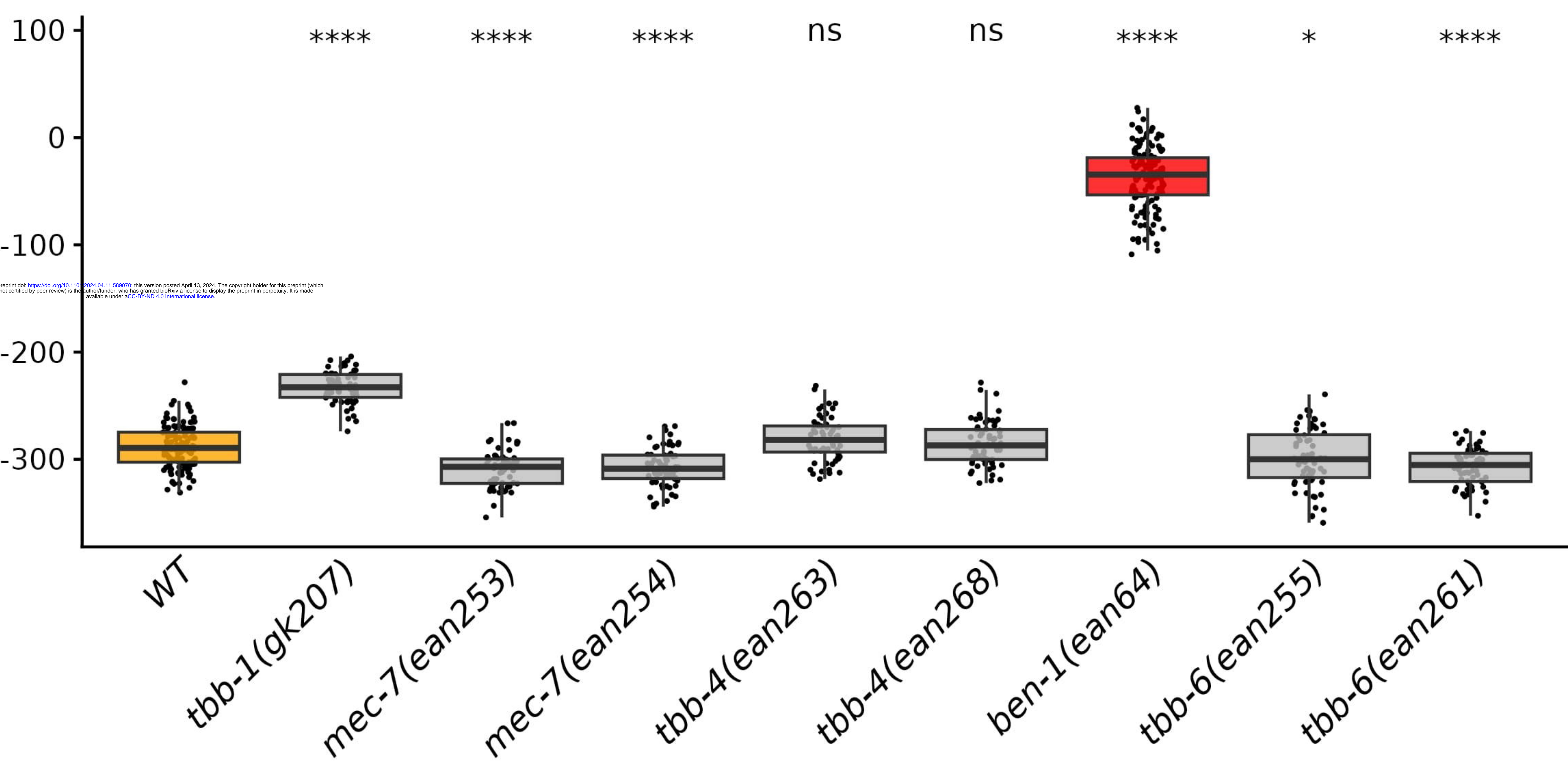


Median animal length





Normalized median animal length



bioRxiv preprint doi: <https://doi.org/10.1101/2024.04.11.589070>; this version posted April 13, 2024. The copyright holder for this preprint (which was not certified by peer review) is the author/funder, who has granted bioRxiv a license to display the preprint in perpetuity. It is made available under aCC-BY-ND 4.0 International license.

Median animal length

900

800

700

\*\*\*\*\*

\*

ns

ns

ns

\*

\*

\*\*\*\*\*

WT

tbb-1(gk207)

mec-7(ean253)

mec-7(ean254)

tbb-4(ean263)

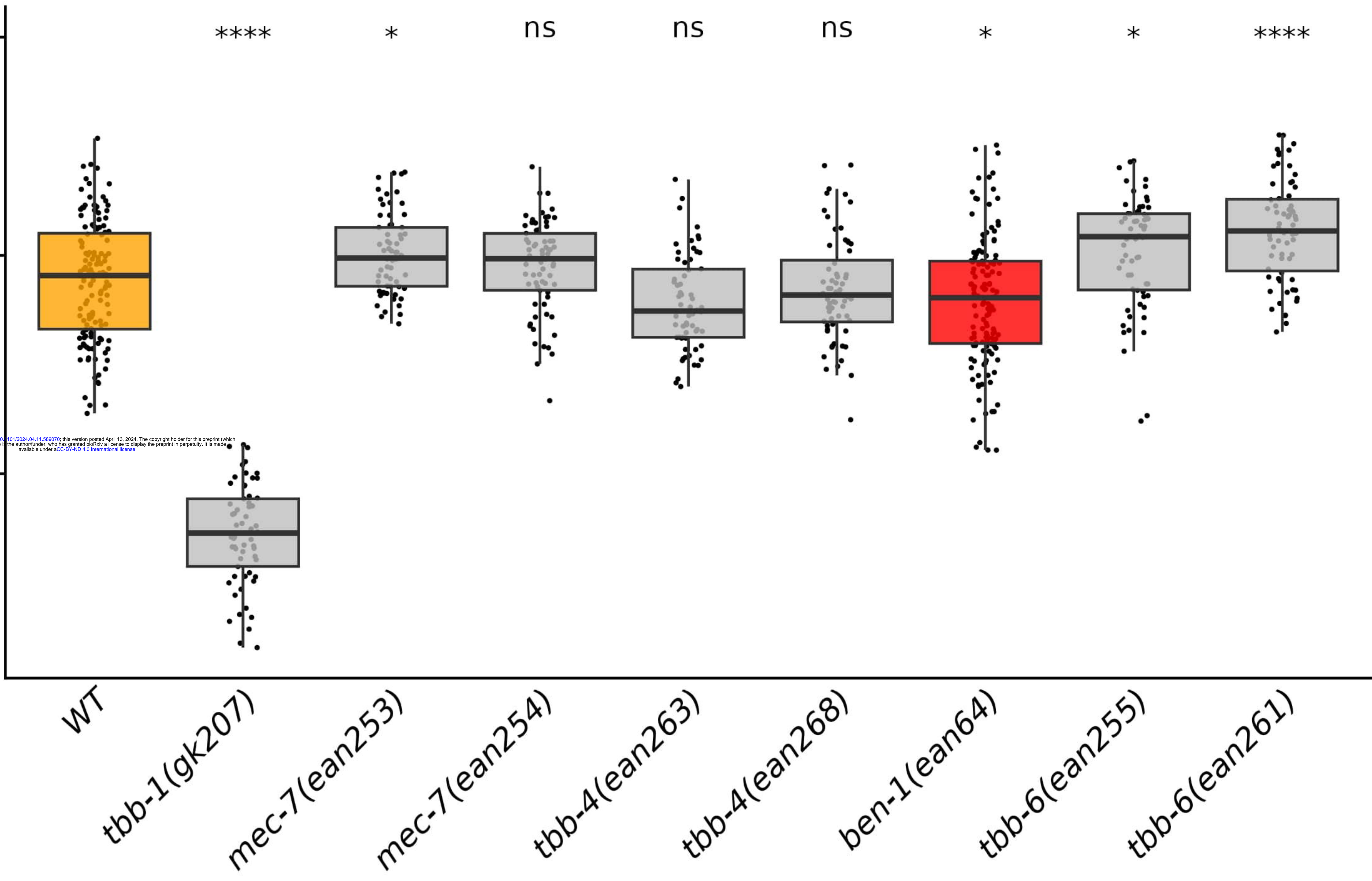
tbb-4(ean268)

ben-1(ean64)

tbb-6(ean255)

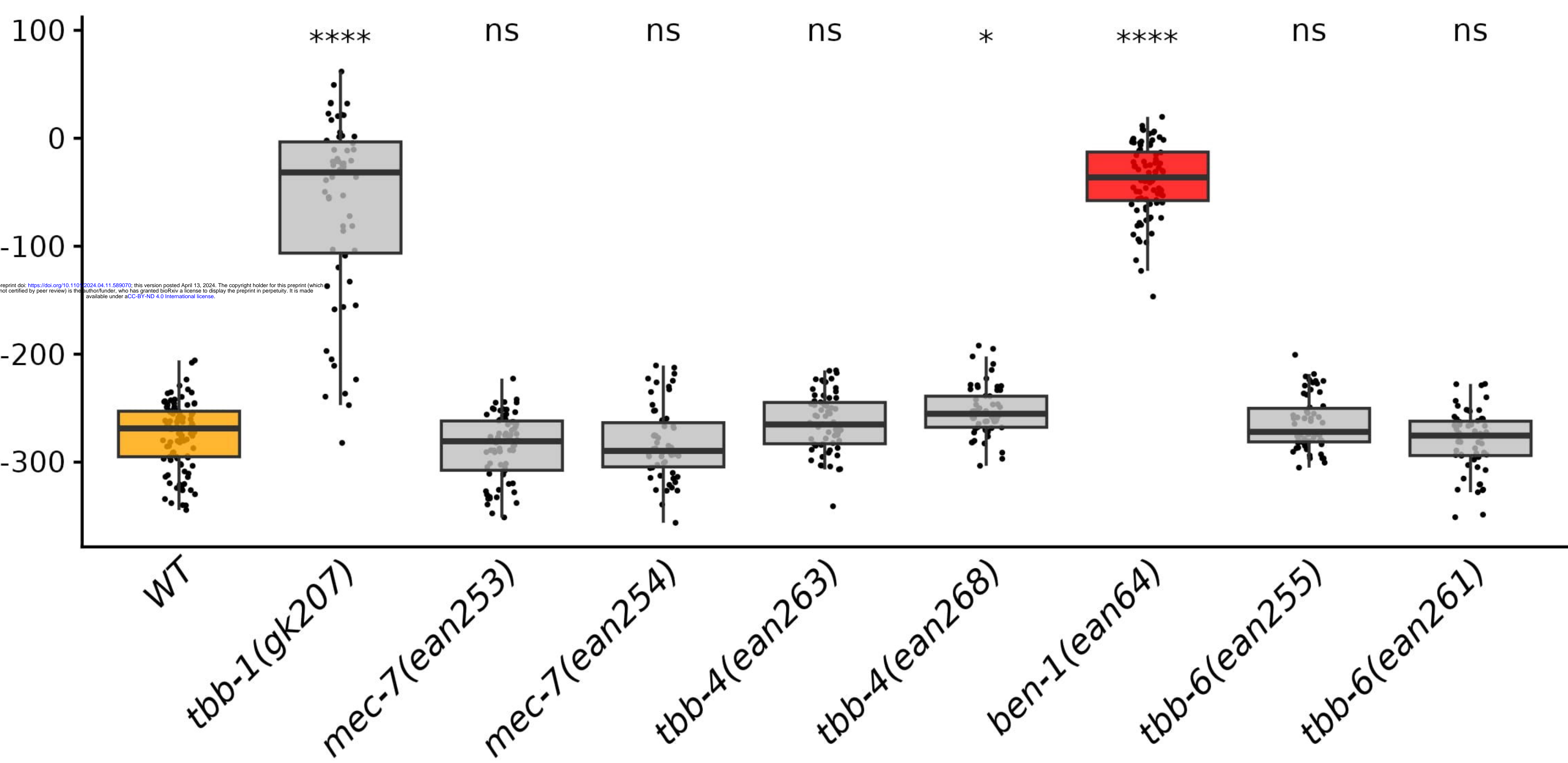
tbb-6(ean261)

bioRxiv preprint doi: <https://doi.org/10.1101/2024.04.11.599070>; this version posted April 13, 2024. The copyright holder for this preprint (which was not certified by peer review) is the author/funder, who has granted bioRxiv a license to display the preprint in perpetuity. It is made available under aCC-BY-ND 4.0 International license.





Normalized median animal length



bioRxiv preprint doi: <https://doi.org/10.1101/2024.04.11.589070>; this version posted April 13, 2024. The copyright holder for this preprint (which was not certified by peer review) is the author/funder, who has granted bioRxiv a license to display the preprint in perpetuity. It is made available under aCC-BY-ND 4.0 International license.

Median animal length

900  
800  
700  
600

\*\*\*\*

ns

ns

ns

ns

ns

ns

\*

WT

tbb-1(gk207)

mec-7(ean253)

mec-7(ean254)

tbb-4(ean263)

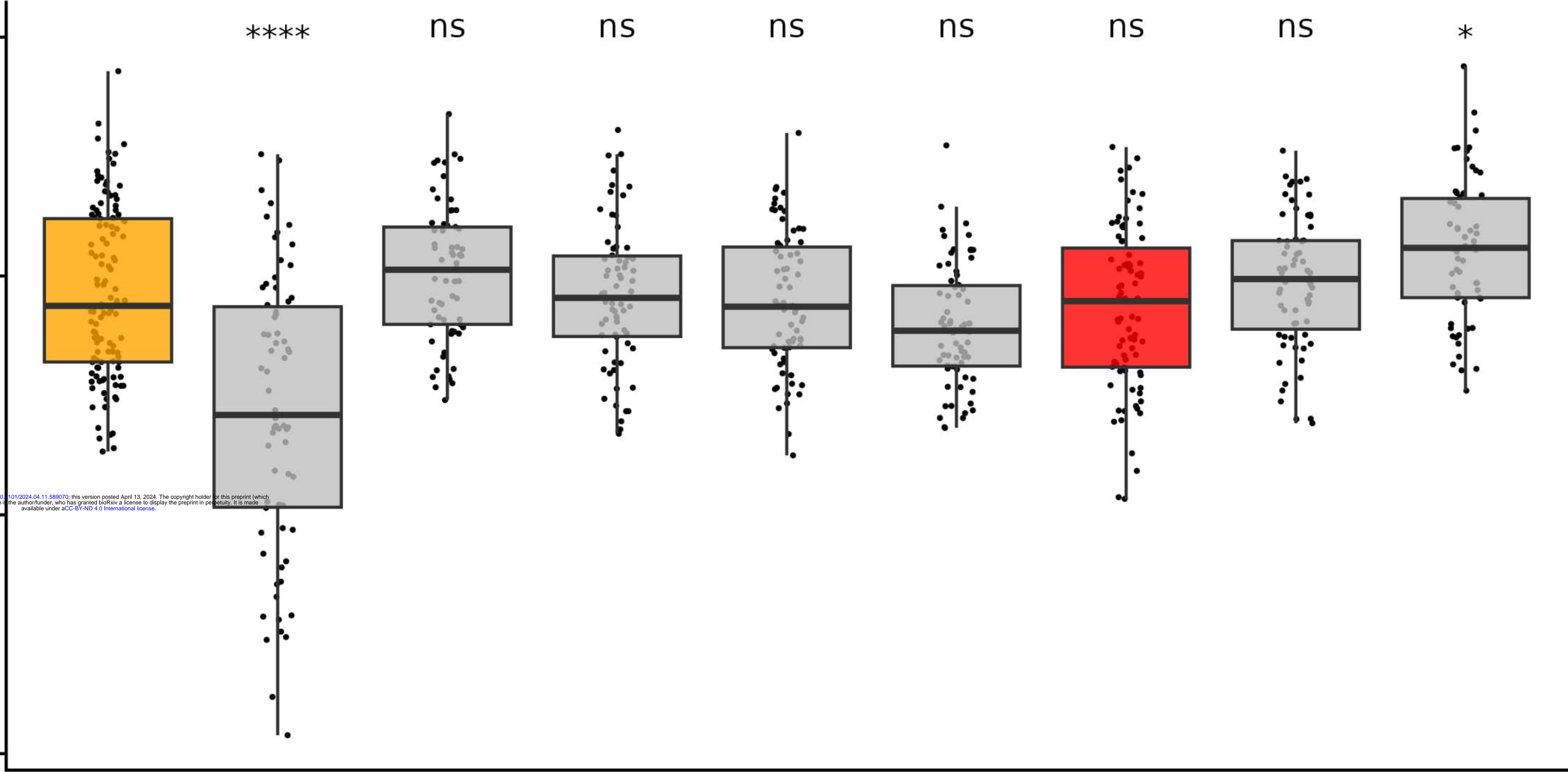
tbb-4(ean268)

ben-1(ean64)

tbb-6(ean255)

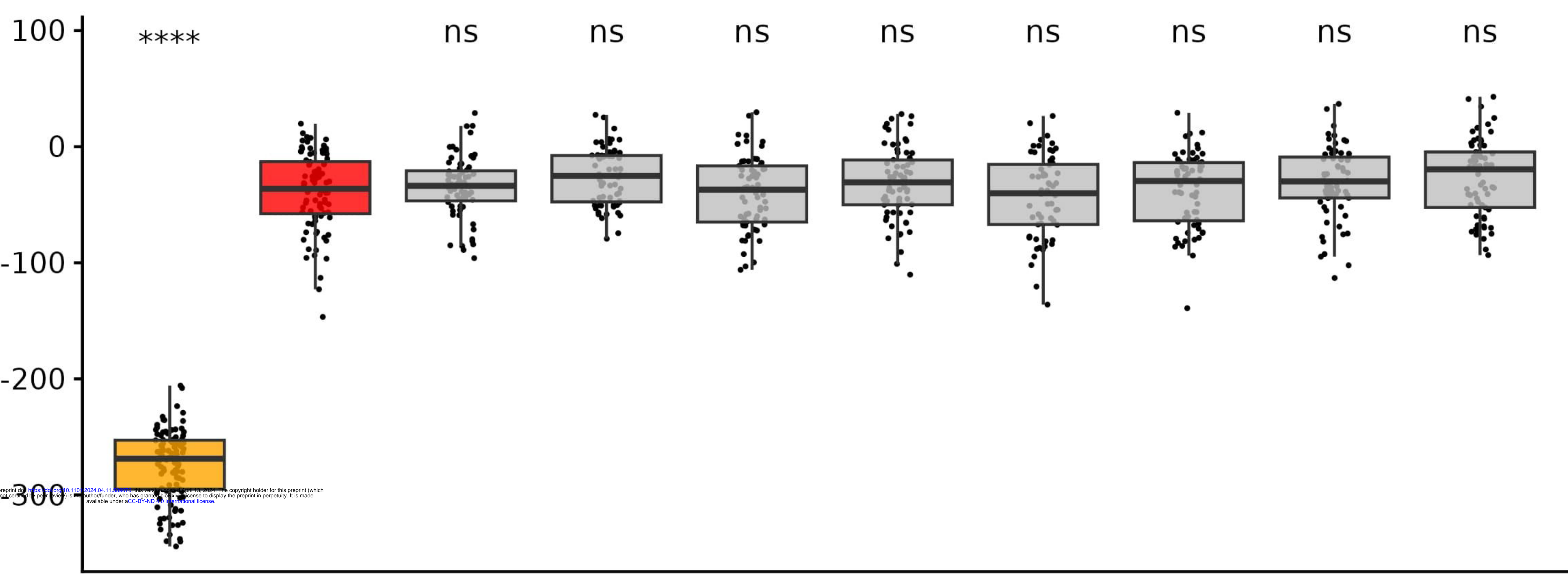
tbb-6(ean261)

bioRxiv preprint doi: <https://doi.org/10.1101/2024.04.11.599070>; this version posted April 13, 2024. The copyright holder for this preprint (which was not certified by peer review) is the author/funder, who has granted bioRxiv a license to display the preprint in perpetuity. It is made available under aCC-BY-ND 4.0 International license.





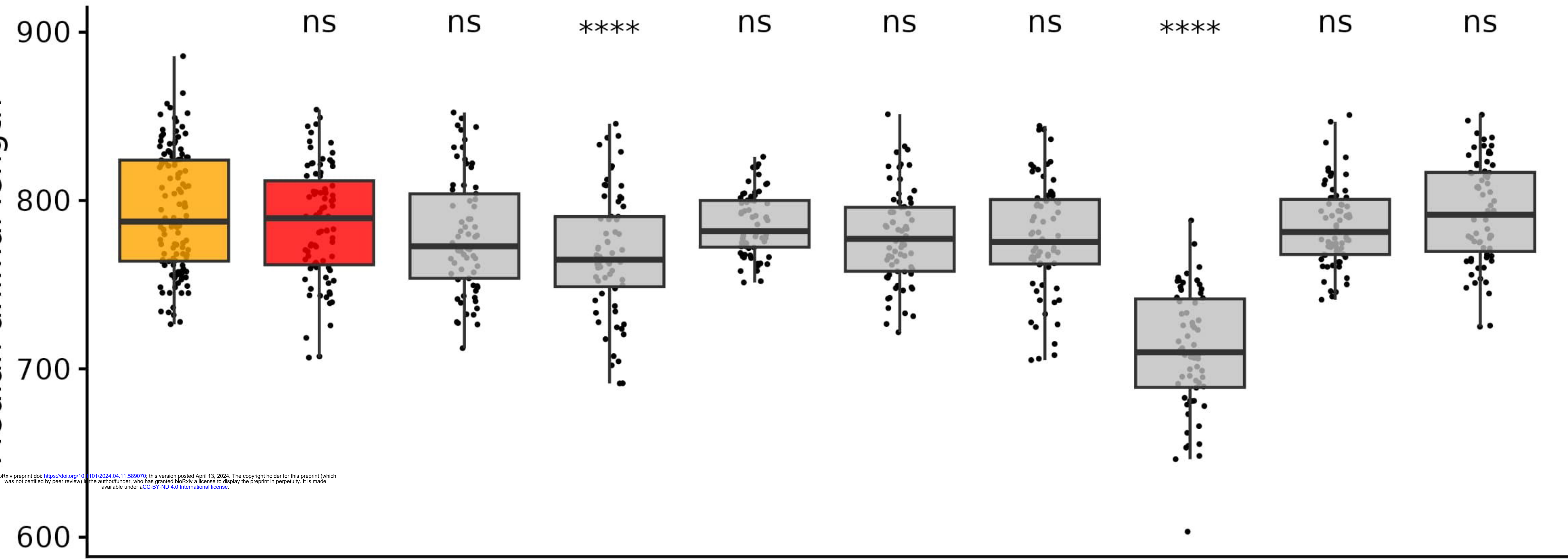
Normalized median animal length



bioRxiv preprint doi: <https://doi.org/10.1101/2024.04.11.899999>; this version posted April 11, 2024. The copyright holder for this preprint (which was not certified by peer review) is the author/funder, who has granted bioRxiv a license to display the preprint in perpetuity. It is made available under aCC-BY-ND 4.0 International license.



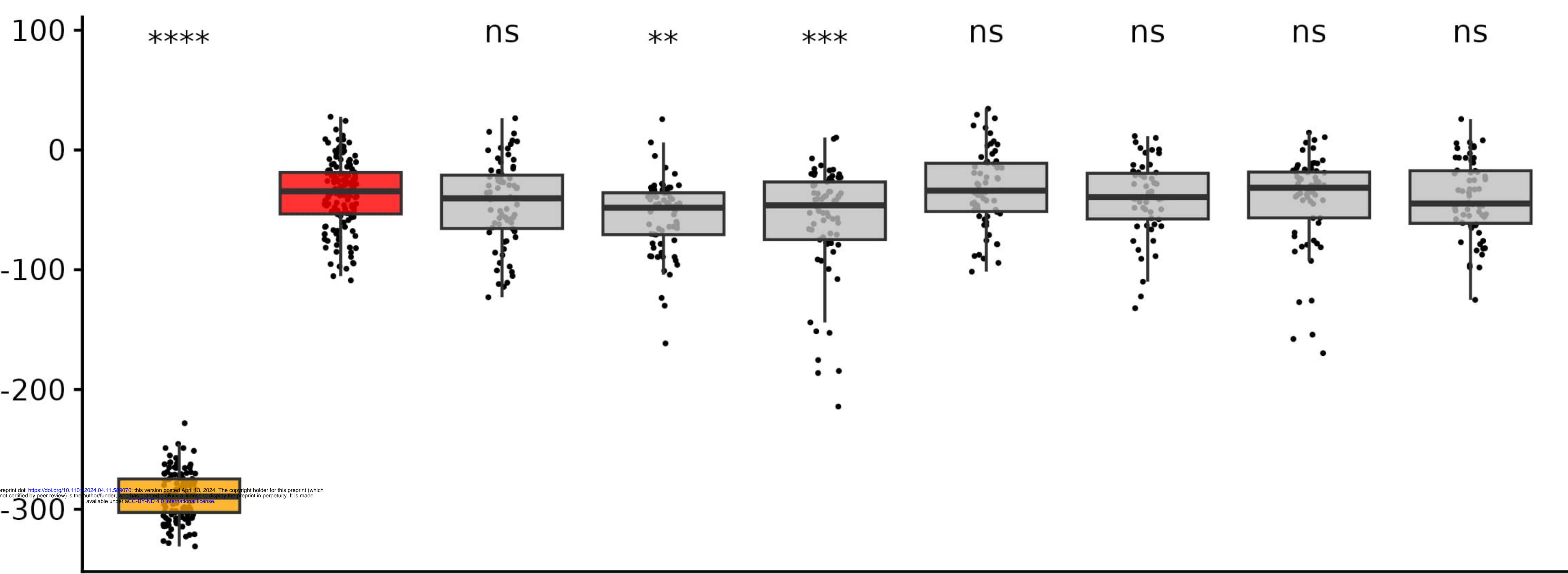
Median animal length



bioRxiv preprint doi: <https://doi.org/10.1101/2024.04.11.599070>; this version posted April 13, 2024. The copyright holder for this preprint (which was not certified by peer review) is the author/funder, who has granted bioRxiv a license to display the preprint in perpetuity. It is made available under aCC-BY-ND 4.0 International license.



Normalized median animal length





Median animal length

900  
800  
700

ns \*\*\* ns ns ns \*\*\*\* ns ns

WT  
ben-1(ean64)  
ben-1(ean64) tbb-1(ean285)  
ben-1(ean64) tbb-1(ean286)  
ben-1(ean64); mec-7(ean258)  
ben-1(ean64); tbb-4(ean262)  
ben-1(ean64); tbb-4(ean282)  
ben-1(ean64); tbb-6(ean259)  
ben-1(ean64); tbb-6(ean260)

bioRxiv preprint doi: <https://doi.org/10.1101/2024.04.11.599070>; this version posted April 13, 2024. The copyright holder for this preprint (which was not certified by peer review) is the author/funder, who has granted bioRxiv a license to display the preprint in perpetuity. It is made available under aCC-BY-ND 4.0 International license.

